GEAP-13539-11
AEC Research and
Development Report
December 1969

SODIUM TECHNOLOGY DEVELOPMENT PROGRAM
MASS TRANSFER INVESTIGATIONS IN LIQUID METAL SYSTEMS

Quarterly Progress Report No. 11
September–November 1969

Approved: R.S. Young
R.S. Young, Project Engineer
Sodium Mass Transfer Program

Approved: E.L. Zebroski
E.L. Zebroski, Manager
Sodium Reactor Technology Section

Prepared for the
United States Atomic Energy Commission
Contract No. AT(04-3)-189
Project Agreement 15

Printed in U.S.A Available from the
Clearing House for Federal Scientific and Technical Information
National Bureau of Standards, U.S. Department of Commerce
Springfield, Virginia
Price: $3.00 per copy

BREEDER REACTOR DEVELOPMENT OPERATION
GENERAL ELECTRIC
SUNNYVALE, CALIFORNIA

6030 SRT 30
175 GJW I/70

DISCLAIMER

LEGAL NOTICE

This report was prepared as an account of Government sponsored work. Neither the United States, nor the Commission, nor any person acting on behalf of the Commission:

A. Makes any warranty or representation, expressed or implied, with respect to the accuracy, completeness, or usefulness of the information contained in this report, or that the use of any information, apparatus, method, or process disclosed in this report may not infringe privately owned rights; or

B. Assumes any liabilities with respect to the use of, or for damages resulting from the use of any information, apparatus, method, or process disclosed in this report.

As used in the above, "person acting on behalf of the Commission" includes any employee or contractor of the Commission, or employee of such contractor, to the extent that such employee or contractor of the Commission, or employee of such contractor prepares, disseminates, or provides access to, any information pursuant to his employment or contract with the Commission, or his employment with such contractor.

TABLE OF CONTENTS

LIST OF ILLUSTRATIONS

LIST OF TABLES

1. INTRODUCTION AND PROGRAM SUMMARY

1.1 GENERAL

Corrosion of candidate structural materials, the effects of corrosion on the mechanical properties, and sodium impurities are being studied in test loops designed to simulate typical conditions of sodium cooled reactors. The program is designed to obtain out-of-pile test data that will permit optimum material selections (when used in conjunction with irradiation data) and the establishment of corrosion and sodium purity specifications for large plants. The work is in support of the Liquid Metal Fast Breeder Reactor (LMFBR) and the Fast Flux Test Facility (FFTF) development programs.

In an earlier 6-year phase of the program ending in 1965, corrosion and mass transfer of type 316 stainless steel and 2-1/4Cr-1Mo and 5Cr-1/2Mo-1/2Ti ferritic steels were studied in depth at sodium temperatures to 1200°F. More than 2500 samples of these materials were exposed to sodium during a total of 140,000 hours of loop operations. Average corrosion rates were correlated by statistical analysis from which quantitative relations were derived. The data were correlated with the variables of temperature, sodium velocity, sodium impurity content under cold trap control, and type of material.

In the current phase of the program, the number of materials studied has been extended to include cladding candidates for oxide fuel (types 304, 316, and 347 stainless steels (SS), and incoloy 800). The temperature range of testing has been increased to 1300°F, and temperature profiles, loop geometry, and sodium purity controls have been established to represent environments of large fast reactors in an improved way.

1.2 SUMMARY OF TASKS

The Sodium Mass Transfer Program is organized into five tasks. These tasks and their objectives are as follows:

Task I: Corrosion and Deposition

Objectives are improvements of empirical and rational models for the accurate prediction of corrosion and mass transport in primary and secondary sodium systems of large plants.

Task II: Sodium Impurities Determinations and Particulate Impurity Identification

This task has the objectives of developing improved methods for sampling of sodium systems, impurity monitoring, collection and identification of particulate material, and chemical and structural analysis. An operating objective is to provide well-controlled operation of loops and to support the development of rational models.

Task III: Ferritic Material Evaluation

This task has the objective of defining program needs and experimental requirements for the application of ferritic steels to LMFBR systems. No work is currently underway on this task.

Task IV: Corrosion and Mass Transport Effects on Composition, Structure, and Structural integrity of Candidate Alloys for LMFBR's and Localized Attack

The objective is to obtain exposures of specific LMFBR candidate materials, including types 304 and 316 stainless steel tubing, and to determine correlations between mass transfer and sodium impurity effects which affect long term stress rupture properties.

Task V: Large System Correlations

The purpose of this task is the correlation of corrosion data from a large sodium system with predictions from corrosion models developed in task I. Sample holder assemblies are installed in the Sodium Components Test Installation (SCTI) for this purpose.

Task VI: Evaluation of Mass Transfer State-of-the-Art and Analysis of FFTF Fuel Cladding, Piping, and Closed Loop Material Degradation Rates

The objective of this task is to provide the basis for selection of allowances for materials degradation of selected FFTF components over the life of the plant. This task is complete and a report is in preparation.

1.3 SUMMARY OF SIGNIFICANT RESULTS DURING REPORTING PERIOD

1.3.1 Task I: CORROSION-DEPOSITION STUDIES

A test run (8-5) in loop 8 at 1300°F was completed and the samples were removed from the loop and processed. The run is designed to give corrosion data for a 30-inch core test section at a sodium velocity of 21 ft/sec. The tubular samples in this section are exposed to sodium on both surfaces to eliminate effects of crevices and to permit quantitative evaluation of downstream (saturation) effects.

Fabrication of corrosion specimens reached 90% completion for test run 8-6. This run is directed toward the study of the effects of high oxygen concentrations on formation of particulates and carbon transport.

Test run 9-2a was started to provide corrosion data at high oxygen levels (30-50 ppm) and to study the efficiency of a cold trap which is magnetically stirred. Initial tests indicate about a four-fold improvement in rate of hydrogen removal from the loop as indicated by a diffusion cell.

Pure nickel exposed to hot-leg sodium in loop 9 at $\approx$ 1200°F ($<$ 10 ppm oxygen) was observed to corrode (-4.3 mils/yr) about 20 times more than adjacent samples of type 304 stainless steel (-0.21 mils/yr). Examination showed severe intergranular penetration (2 mils) in 1300 hours.

The examination of deposits taken from different regions of nonisothermal loops has given insight into the mechanism of mass transport and deposition. The amount of chromium and nickel which is transported and removed from the sodium as it is cooled is enhanced by the formation of particulates beyond that which would be expected from the temperature dependence of solute solubility alone.

1.3.2 Task II: SODIUM IMPURITIES

A negligible effect on oxygen contamination of a loop during sampling of sodium was confirmed. An estimate of the amount of contamination added to loop 8 during exchange of rapid samplers was made by observing the change in reading of an oxygen meter. An increase of $\leqslant$ 1 ppm oxygen was indicated upon valving in a new sampler, and this was reduced to the original level after 1-½ hours of flow through the sampler and normal cold trapping.

A second experiment involving the collection of plugging material (using a specially designed plugging indicator) was done in a loop that showed only a single flow break at low temperature. This verified a second time that the predominant impurity contributing to plugging in this loop was sodium hydride.

Initial attempts to isolate chemical species at trace levels in particles collected by filtration from loop 1R (predominantly alpha iron) showed no new phases when bromine-methanol solutions were used to wash residue from the filter. X-ray diffraction showed a loss of carbide phase (M_7C_3) because of the treatment.

An initial trial of on-line distillation (on the 1 kg scale) to concentrate particulate impurities was not quantitative because of occasional carryover. About 7 mg of residue were obtained. Sodium carbonate was the major constituent; small amounts of α-iron and a compound of the form $NaMO_2$ also were observed.

1.3.3 Task IV: CORROSION AND MASS TRANSPORT EFFECTS ON STRUCTURAL INTEGRITY

Additional exposure time in sodium at 1300°F and 1150°F was obtained for candidates for LMFBR cladding, including stressed specimens in three test loops (to observe mass transfer effects on microstructure and on structural integrity.)

Loops 4R, 5R, and 6R operated for 1252, 1689, and 1844 hours, respectively, during the report period. Nine failures of pressurized specimens were logged extending the time-to-rupture data to 5187 hours at 1300°F and 1947 hours at 1150°F.

Control tests in argon at 1300°F have been extended to 3389 hours. A significant decrease in stress-rupture properties due to exposure to nonisothermal flowing sodium is indicated.

Review of circumstances and examination of specimens from task F, P.A. 10 capsule tubes that had been irradiated in EBR-II (which in one instance showed localized intergranular attack) revealed sensitization of the type 304 stainless steel. The observed sensitization (disintegration of samples in a Strauss test) indicated a carbon pickup of the capsule tubes.

1.4 REPORTS

Monthly report letters are prepared reporting progress in all tasks. Progress letters through October 31, 1969 have been issued.

Topical reports and quarterly progress reports issued covering test results are listed in section 5.

2. TASK I: CORROSION-DEPOSITION STUDIES

2.1 GENERAL

This work is directed toward the following:

- experimental study of the corrosion of steel, including types 304 and 316 stainless, exposed to flowing sodium at bulk temperatures to 1300°F
- development of an understanding of the mechanisms involved in the phenomena of corrosion, mass-transport, and deposition in small test loops so that extrapolations can be made to larger systems
- monitoring of the test systems for localized attack
- establishment of relationships between sodium impurities, loop operations, and metallurgical effects
- using heaters employing heat flux of 0.5 to 1.0 x 10^6 Btu/h-ft^2 average in sodium to measure the effects of reactor heat flux on materials

The work is carried out in test loops constructed to simulate corrosion conditions of a 1000 MW coolant system and a closed loop system for FFTF.

2.2 OPERATION OF TEST FACILITIES

A summary of loop operations including conditions of tests and operating times is shown in table 1 for the 3 month period ending November 14, 1969.

2.3 LOOP 8 PARAMETER STUDY

A test run (8-5) completed last period was designed to obtain quantitative data on the downstream (saturation) effect on corrosion rate at 1300°F and low oxygen ($<$ 10 ppm). The test run (8-6) in preparation is designed to extend the data to higher oxygen levels ($\approx$ 30 ppm) and for study of the effect on formation of particulates and subsequent transport of carbon species from hot to cold-leg areas.

The following activities were carried out in the current report period.

- removed and processed run 8-5 samples
- fabricated run 8-6 samples to 90% completion
- fabricated parts for a second cold trap to be placed in parallel with original cold trap and operated to establish effectiveness of oxygen control. The No. 1 cold trap will be spiked with a large inventory of Na_2O in order to provide sufficient oxygen source during the run. Preparation for modifying the No. 1 trap was in progress during this period.
- performed maintenance and overhaul of in-line distillation equipment.

2.4 LOOP 9 CHEMISTRY CONTROL STUDY

The purpose of this run (9-2a) is to obtain corrosion data at oxygen levels of about 30 ppm and to determine relationships between cold-trap operation and changes in chemistry of the system.

Run 9-2A started on October 20, 1969 when hot-leg temperatures and loop Δ T were established. During this quarter the following activities were carried out as part of run 9-2A:

- completed connections and checkout of on-line chromatograph installation to the cover gas system of loop 9.
- installed a second cold trap for use in experiments aimed at determining whether increasing Reynold's number in the cold trap by electromagnetic stirring will increase the efficiency for trapping out hydrogen.
- installed a diffusion tube similar to an electron bombardment (EB) heater in the loop to act as a hydrogen detector during cold trap experiments.
- loaded 400 corrosion samples for run 9-2A.

During run 9-2A initial hydrogen control experiments have shown the following:

- the ion pump on the diffusion tube shows a prompt response to increase and decrease in cold-trap temperature. The chromatograph response is much slower, being influenced by the pumping rate, sampling delay time and the slower kinetics in the cover gas phase as compared to the sodium side.
- stirring the cold trap (calculated Reynolds Number, N_R = 13.8 x 10^5) produced about a four-fold

TABLE 1

SUMMARY OF LOOP OPERATIONS

Conditions of Test

	Temp (°F)	ΔT (°F)	Flow (gpm)	T_s* or CT** (°F)	Time (hours)
Run 8-6	1,300	500	5.7	<470	2,000
	Three month operation				0
	Cumulative (run 8-6)				0
	Total loop age				21,189
Run 9-2A	1,300	500	5	<425	2,000
	Three month operation				996
	Cumulative (run 9-2A)				673
	Total loop age				14,244
Run 1R-1	1,300	500	2	<300	----
	Three month operation				1,604
	Cumulative (run 1R-1)				3,768
	Cumulative (run 1R-2)				24
	Total loop age				4,438
Run 4R-2	1,300	500	8	<300	10,000
	Three month operation				1,252
	Cumulative (run 4R-2)				
	1,000° and above				6,424
	1,300° and pressure applied				6,064
	Total loop age				8,333
Run 5R-5	1,300	500	10	<300	5,000
	Three month operation				1,689
	Cumulative (run 5R-5)				
	1,000°F and above				1,356
	1,300°F and pressure applied				1,259
	Total loop age				16,471
Run 6R-4	1,150	440	10	<300	10,000
	Three month operation				1,844
	Cumulative (run 6R-4)				
	1,000°F and above				2,784
	1,150°F and pressure applied				2,261
	Total loop age				9,162

NOTE: for the period of Aug. 24—Nov. 14, 1969

*T_s = Plugging Temperature

**CT= Temperature of Cold Trap

improvement in rate of hydrogen removal as monitored by the in-sodium hydrogen detector.

- the effect of stirring versus nonstirring on cover gas hydrogen is not yet clear. The cold-leg hydrogen decreased at almost the same rate for either case, whereas the hot-leg hydrogen decreased less rapidly in the stirred mode.

- stirring appears not to influence the N_2 level in the cover gas.

Vanadium and niobium wires obtained from Argonne National Laboratory (ANL) were exposed in the hot leg of loop 9 early in run 9-2a. The wires were fastened in a flow-through sampling tube and exposed for 7 hours at a sodium temperature of about 1220°F. Upon removal from the loop, a section of the tube with sodium frozen in place was cut off each end under dry argon conditions ($\approx$ 0.5 ppm H_2O and $\approx$ 1 ppm O_2) for impurity determinations, and the remaining section with wires was capped and packaged for shipment to ANL. The wires will be used in internal friction measurements and determination of oxygen in the sodium.

2.5 LOOP 1R: PARTICULATE STUDY

Run 1R-2: 1300°F (T max), 800°F (ΔT), 300°F (Ts), 1000 Hours.

The objective of this test is to generate, collect, and analyze relatively large quantities of particles of corrosion products under controlled conditions, and develop a basic understanding of their role in sodium mass transfer.

During this quarter the loop was operated on run 1R-1 at temperatures of 1300°F maximum in the hot leg and 500°F in the cold leg. The flow was 2 gpm until October 21 when the loop was shut down for removal of the 5μ filters and a magnetic particle collection (MPC) pipe from the cold leg. The flow tube was X-rayed; it is not apparent from the X-ray that there are any magnetic particles trapped in this region. Both the flow tube and filter are being examined further.

Following replacement of the MPC pipe, the loop was restarted for a 2-day cleanup run, then the new 10μ filter was installed. The loop is presently at run 2 condition of 1300°F, 2 gpm - operating at substantially lower pump power. No significant flow change caused by particulate buildup is apparent.

2.6 RATIONAL MODEL STUDIES

Corrosion of stainless steel in a sodium system is a function of velocity or conditions of flow such as fluid boundary layers or Reynold's numbers that are associated with the geometry of the system. Reactor systems of the LMFBR type will operate with Reynold's numbers up to the order of 100,000. Thus, to obtain scale up test data or extrapolate from small test loops with Reynold's numbers on the order of 30,000, an experiment test loop has been designed to reproduce boundary layer conditions typical of large systems. The high Reynold's numbers will be obtained by rotating specimen surfaces in a flowing stream of sodium with oxygen activity control by electro-chemical cells. Basic design parameters of the loop were given in quarterly report No. 10 (GEAP-13539). Detail design of the test set-up was completed in November. All equipment and materials for construction were placed on order and fabrication of some components started.

2.7 CORROSION DATA ANALYSIS

In order to study the corrosion behavior of nickel, a few pure nickel samples were inserted in run 9-2 for about 1300 hours. The local velocity and temperature of the sodium were $\approx$ 2 ft/sec and 1200°F, respectively. The oxygen level was maintained at $<$ 10 ppm. The corrosion rate of pure nickel (-4.3 mils/year) was about 20 times higher than adjacent type 304 stainless steel (-0.21 mils/year).

United Kingdom observations show that at sodium velocities of 30 to 40 ft/sec, containing 20 to 30 ppm of oxygen, the corrosion rate for pure Ni (-3.9 mils/year) at 1202°F is only about two times higher than type 316 stainless steel (-1.8 mils/year).

The higher corrosion rate for nickel is believed to be caused by the rapid rate of intergranular dissolution of nickel. The metallographic observations of the pure nickel sample (figure 1) showed severe intergranular penetration (2 mil) in 1300 hours at $\approx$ 1200°F. This observation is consistent with previously observed intergranular penetration of high nickel base alloys. Metallurgical and chemical analyses of the specimens from runs 8-5 and 9-2 are in progress.

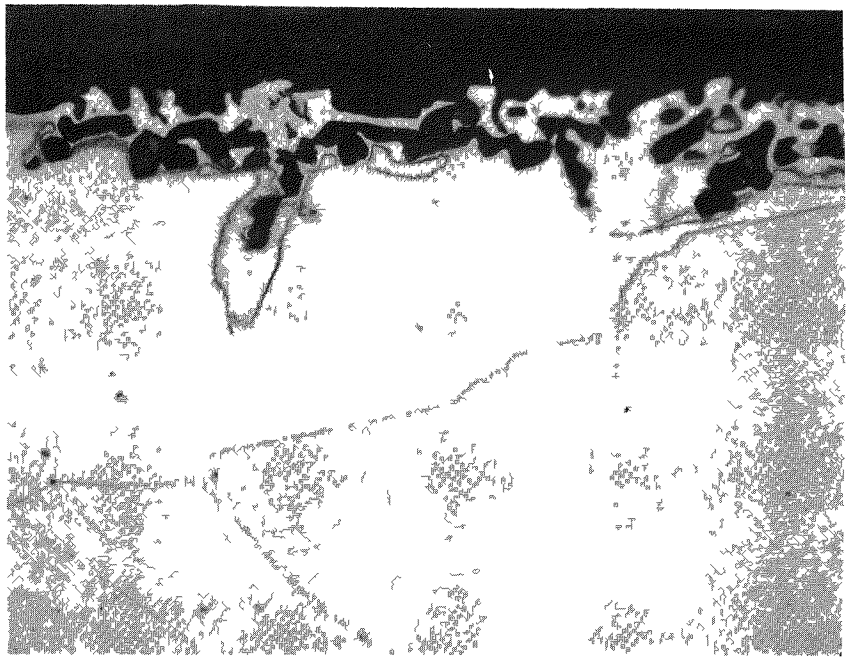

Figure 1. Pure Nickel Sample after Exposure of 1300 hours at ≈ 1200°F.

2.8 NATURE OF THE PARTICULATES IN LOOP SODIUM

Recent experimental evidence suggests that the corrosion and deposition processes in a flowing nonisothermal sodium system are interdependent, and each exerts considerable influence over the extent and characteristics of the other. Therefore, a performance analysis of nonisothermal sodium systems must consider these processes as complementary and equal in significance to the overall system behavior.

In order to explore the factors which influence the composition and structure of particulates (deposits) and the location and rate at which they are deposited, deposits from several areas have been removed from experimental facilities for study. An analysis has been completed on particulates collected from (a) corrosion specimens positioned in the initial regions of cooled sections of the test loops (1200° - 1070°F), (b) the piping of an economizer (300° - 700°F), and (c) a nickel filter (600°F).

Identification of the species of the particulates (composition and structure) deposited in flowing nonisothermal systems should provide insight into the influence of temperature, temperature gradient, impurity level, and flow characteristics of the sodium on the following:

- the mechanisms of the corrosion and deposition processes (in particular, the rate-controlling steps)
- the predominant species involved in the mass transfer process
- the morphology of the particulate and the nature of the bond to the substrate (and, by inference, the long-term effect upon heat transfer characteristics of the component)
- the probable distribution of radioactive corrosion products throughout the primary system of a reactor
- potential approaches to controlling the rate, amount, and location of deposition

The compositions of the deposits removed from the various loop positions are listed in table 2. These values are believed to be accurate to within ± 10% of the value stated. In addition to the elements shown in table 2, trace concentrations of cobalt, molybdenum, magnesium, silicon, and tin were observed in the spectrographic analyses. The balance of each deposit is assumed to be predominately oxygen.

The x-ray diffraction analysis of the deposits from impingement samples, particulate residue from economizer, and particulates from the nickel filter are shown in tables 3, 4 and 5, respectively.

2.9 DISCUSSION

The physicochemical properties of the deposits formed in a nonisothermal system of flowing sodium are a direct

TABLE 2

ELEMENTAL COMPOSITION OF VARIOUS DEPOSITS

Source (and Temperature) of Deposit	Element (%) Fe	CR	Ni	Na	Mn	Si	Ca	C
Impingement Cartridge (1,070°F)	6	35	25	10	7	---	---	~3
Economizer (300°-700°F)	21	13	10	14	---	6	---	---
Ni Filter (600°F)	10	7	2	42	3.3	5.5	1.1	~2

---Analysis not performed

TABLE 3

X-RAY DIFFRACTION ANALYSIS OF DEPOSIT FROM IMPINGEMENT SAMPLES (1,070°F)

Constituent	Structure	Lattice Constants	Relative Concentration
Austenitic Phase	Face Centered Cubic	a_o = 3.586 ± 0.009 A	Major
$M_{23}C_6$	Face Centered Cubic	a_o = 10.629 ± 0.009 A	Strong Minor
M_7C_3	Hexagonal	a_o = 13.98 ± 0.02 A c_o = 4.523 ± 0.007 A	Minor
$NaMO_2$	Hexagonal	a_o = 2.969 ± 0.007 A c_o = 15.909 ± 0.007 A	Minor
Fe_3C, α-Fe, α-Mn, Cr			Trace

TABLE 4

X-RAY ANALYSIS OF PARTICULATE RESIDUE FROM ECONOMIZER (300°-700°F)

Constituent	Structure	Lattice Constants	Relative Concentration
Alpha Iron	Body Centered Cubic	a_o = 2.869 ± 0.007 Å	Major
$M_{23}C_6$	Face Centered Cubic	a_o = 10.685 ± 0.009 Å	Weak Minor
M_7C_3	Hexagonal	a_o = 14.045 ± 0.009 Å c_o = 4.556 ± 0.009 Å	Trace
$NaMO_2$	Hexagonal	a_o = 2.969 ± 0.007 Å c_o = 15.909 ± 0.007 Å	Trace
M_3C_2	Orthorhombic	a_o = 11.46 ± 0.01 Å b_o = 5.52 ± 0.01 Å c_o = 2.82 ± 0.01 Å	Trace

TABLE 5

X-RAY DIFFRACTION ANALYSIS OF PARTICULATES FROM NICKEL FILTER (600°F) WHICH WERE INSOLUBLE IN WATER

Constituent	Structure	Lattice Constants	Relative Concentration
Alpha Iron	Body Centered Cubic	a_o = 2.869 ± 0.007 Å	Major
Austenitic Phase	Face Centered Cubic	a_o = 3.588 ± 0.005 Å	Strong Minor
$M_{23}C_6$	Face Centered Cubic	a_o = 10.623 ± 0.005 Å	Trace
M_7C_3	Hexagonal	a_o = 13.98 Å c_o = 4.523 Å	Trace

function of the temperature at which the deposit is formed. In the higher-temperature regions (1000° to 1200°F) the deposited material has a well-defined crystalline appearance and is rich in chromium and nickel. In the lower-temperature regions (<1000°F), the deposit is rich in iron and irregular in appearance.

The mechanism of deposition in the higher-temperature regions probably involves the formation of particulates (distinct chemical compounds, such as the complex carbides and sodium chromite, with characteristic lattice structures) in the sodium stream prior to deposition, and the subsequent accumulation of these particulates on the substrate material. Through the formation of particulates, the amount of chromium and nickel which is removed from the sodium as it is cooled is enhanced beyond that which would be expected from the temperature dependence of solute solubility alone. The driving force for chromium to deposit in these regions is also independent of the composition of the substrate material.

The mechanism of deposition at the lower temperatures most probably involves the diffusion of solute atoms (primarily iron) across the liquid boundary layer onto the substrate material.

The transport of carbon, through the formation of chromium carbide particulates in the sodium stream, contributes to the carburization of substrate material in the cold leg of an entirely austenitic system.

The potential for mass transfer from material in the hot leg of a sodium system is directly dependent upon the difference in the activity of the solutes in the material and in the sodium.

Pure iron samples exhibited extensive grooving at grain boundaries in the high-temperature corrosion regions of the loop. Stainless steel specimens formed a ferritic surface phase because of selective elemental leaching, and the ferritic phase showed grooving at the grain boundaries which was similar to that observed on the pure iron samples.

A large amount of silicon was present in the cold leg deposits, probably due to selective leaching from stainless steels in the hot leg.

Particulates in suspension in sodium may be the reason for the discrepancy between "solubility" data and the chemical analyses of the loop sodium, which is usually an order of magnitude higher.

The presence of $NaCrO_2$ and $M_{23}C_6$ is consistent with the available thermodynamic data. The absence of ternary metal oxides (e.g., $NaMO_2$ with the M cation consisting of iron and nickel) below 10 ppm oxygen in sodium is also in agreement with the calculated thermodynamic stabilities of these compounds.(0)

3. TASK II: SODIUM IMPURITY INTERACTIONS AND IDENTIFICATION OF PARTICULATE MATTER

Work in this task encompasses the extensive support in sodium chemistry, sodium and gas sampling from loops, impurities detection, and control required primarily by task I of this program.

3.1 LOOP MONITORING FOR IMPURITIES

3.1.1 FLOW-THROUGH SAMPLING, IN LINE

The method used for obtaining samples on a regular basis, normally biweekly, representative of loop sodium, consists of installing "flow through samplers" made up of lengths of stainless steel tubing, ½-inch o.d., at appropriate points in a test loop. The design and use of these samplers was initially reported in quarterly report No. 2, (GEAP-5546).

3.1.2 TOTAL ALKALINITY MEASUREMENTS

Table 6 provides recent data on the total alkalinity (amalgamation determination) for loop samples.

The loop 1 results have been consistently high and may be because the sampling has been at too low a temperature (520°F for the cold leg) to permit clean-up of sampling lines.

Sporadic high values (e.g., > 15 ppm) are observed for loops 4 and 6. Determinations for hydrogen are not complete; these may afford an explanation.

The effect on the oxygen level in loop 8 of taking flow through samples was measured. Prior to valving the sampler into the system, the oxygen meter reading was 1.160 volts, equivalent to 5 ppm oxygen. After valving in, the reading decreased to 1.155 volts, equivalent to ⩽ 1 ppm increase in oxygen. In 1-½ hours of flow through the sampler, and with normal system cold trapping, the meter resumed its initial reading.

3.1.3 CALCIUM AND SILICON ANALYSES

Interest in the amounts of calcium and silicon present in the sodium in the loops was engendered by the observation of significant quantities of these elements in the material removed by filtration from loop 1.

TABLE 6

TOTAL ALKALINITY IN LOOP SODIUM (FLOW THROUGH SAMPLES)

Sample No.*	Date Taken	Plugging Indicator Temperature (°F)	Total Alkalinity (ppm)
1R-1-1A	5/4/69	Undiscernable	23
1R-1-3A	9/9/69	Undiscernable	18
1R-1-4A	9/30/69	Undiscernable	21
4R-2-8A	6/27/69	270	19
4R-2-9A	8/8/69	273	17
4R-2-10A	9/20/69	257	9
6R-4-1A	8/13/69	Undiscernable	12
6R-4-2A	9/12/69	Undiscernable	15
6R-4-3A	10/1/69	Undiscernable	16
8-5-4A	5/27/69	Undetermined	12,16
8-5-5A	7/1/69	Undetermined	14
9R-2-18A	5/21/69	238	12
9R-2-19A	7/7/69	Undetermined	>100**
9R-2-20A	7/10/69	545	100

*First number and letter designate loop

**Sampler had a void

The determinations were made by standard spectrophotometric techniques. Results appear in table 7.

The calcium results are in the expected range. The silicon data is the first obtained for these systems. In the past, silicon data has either not been sought or discounted when found, on the grounds of probable contamination during sample preparation, viz., attack on glassware while dissolving the sodium. In the present work (as with the

TABLE 7

CALCIUM AND SILICON DETERMINATION IN LOOP SODIUM (FLOW THROUGH SAMPLERS)

Sample No.	Calcium (ppm)	Silicon (ppm)
1R-1-1A	2.0	0.5
8-5-5A	1.7	0.5
9-2-17B	4.8	0.5

loop 1 particulate analyses), care was taken to avoid the contact of caustic solution with silicacious material; therefore, the data are believed to be valid.

3.1.4 ON LINE INSTRUMENTATION

The on line chromatograph is in operation for the first time on the cover gas system of loop 9. The behavior of the impurities in the loop 9 cover gas was typical for a loop start-up. At isothermal conditions, about 750°F, concentrations of 1000 ppm hydrogen were observed. After heating the loop to test condition, from 800° to 1300°F, the hydrogen concentration dropped to the levels shown in table 8.

The hydrogen values are still higher than normal and are expected to decrease with further operation.

3.1.5 SOLIDS COLLECTORS

A second characterization of the material depositing in plugging indicators at low temperatures has been completed (previous work was reported in the 8th quarterly-GEAP 10008). The collection was made in loop 8 with the cold trap operating at 320°F; it was not possible to obtain plugging with the cold trap set at 300°F or below. At the 320°F temperature, plugging indicator readings were 320°F in the oscillating mode and 280°F in the bare orifice mode. Collection of the material in the solids collector under these conditions again showed NaH to be the major impurity deposited. A trace of NaOH, and, for the first time in these studies, a trace of Na_2O was detected. Based on these two tests it appears that the predominant impurity in these loops under normal operating conditions is sodium hydride.

3.2 ANALYTICAL CHEMISTRY, COMPOUND IDENTIFICATION, INTERACTION STUDIES

TABLE 8

IMPURITIES IN THE LOOP 9 COVER GAS

	Hot Leg	Cold Leg
Hydrogen (ppm)	10	35
Nitrogen (ppm)	50	1600

3.2.1 ANALYTICAL DEVELOPMENT

Attempts to improve the characterization procedures for particulates collected in the loop 1 experiment included the following:

- The nature of the collected particulates is not well known because of the effects of distillation and the subsequent hydrolysis step. Methods for direct examination of the material are being investigated. In one such attempt sodium from one of the filter elements from loop 1 was smeared on a glass slide and positioned in the holder developed for the examination by x-ray diffraction of residue from the solid collectors. Sodium metal was essentially the only phase detected. Apparently the concentration of the impurities was insufficient for detection.

- Attempts at isolating trace species from the particles collected by filtration were initiated. Bromine-methanol solutions were used to wash the predominantly alpha-iron residue obtained from the first loop 1 main housing filter. No additional compounds were detectable by x-ray diffractions as a result of this treatment, although the relative concentration of minor components would increase because of the dissolution of iron.

3.2.2 COMPOUND FORMATION, INTERACTION STUDIES

The attempt to obtain x-ray patterns of known or suspected sodium-metal-oxygen interaction products was continued by carrying out the reaction between Na_2O and Fe in an attempt to produce $(Na_2O)_2 \cdot FeO$. An extremely complex diffraction pattern was produced which does not correspond to any available in the literature. The pattern will be used for reference purposes.

3.3 SEPARATION AND IDENTIFICATION OF PARTICULATE MATERIAL

3.3.1 PARTICULATES FROM LOOP 1 FILTRATION

The previous quarterly report in this series describes material filtered from loop 1 during the period April 23, 1969 to May 19, 1969, about 600 hours (loop operation 750 hours).

Work is in progress on a second main housing filter which saw loop service during the period June 25, 1969 to August 15, 1969, about 1100 hours (loop operation of about 2000 hours). About one gram of material was obtained from the distillation of a single filter element.

Emission spectrographic data indicates the same elemental composition as that obtained for the first main housing filter. Specific colorimetric analyses are being performed to obtain a precise measurement of the composition.

Analyses for calcium indicate that about 0.3% of this element was present. This represents a 1% decrease over that observed in the first filter. Analyses for silicon have also been completed. The data shows a doubling in the concentration over that observed for the first main housing filter, an increase from 5% to 10%. Because the loop has been in operation for about 900 hours prior to the insertion of this filter, it would seem the silicon is due to sources other than contamination during loop assembly, e.g., leaching from the steel.

X-ray diffraction analyses of the washed residue showed alpha-iron to be the main constituent with a lesser amount of austenite present. The data also indicates the absence of detectable amounts of carbides and in this respect differs from the material collected in the earlier portion of the loop run. Specific carbon analyses are required to confirm this observation.

A brief examination of a clean-up filter which saw service in the loop for about 1300 hours from April 23, 1969 to June 21, 1969 has been made. The material from one element was separated by distillation and examined by x-ray diffraction and emission spectrography. The major elemental impurities were silicon, calcium, sodium, and the stainless steel constituents. The diffraction pattern for alpha-iron was predominant but some austenite and possibly a carbide phase of the M_7C_3 type was present. In addition, an unidentified constituent was observed. These results are compatible with those reported for the first main housing filter, and no further work is planned on this material since it probably represents loop debris.

Two experiments in support of the particulate study were also performed. In the first, a blank run was made to determine whether the large amount of silicon observed in the particulates was due to contamination during the distillation step or subsequent handling, or both. A piece of unused filter and some sodium were placed in the distillation system and treated in a manner analogous to that for the used filter. Approximately 0.04 mg of silicon was found for the unused filter as compared to 120 mg for the one that had seen service in loop 1, thus indicating that contamination during analysis was not the source of this element.

The second investigation was into the cause of the observed reduction in flow through the filters with time. One hypothesis has been that the pores of the nickel might have been closing during operation at temperature due to restructuring of the nickel, due to solubility in the hot sodium. Metallographic analysis of both a new filter and a filter which had experienced reduced flow showed no apparent change in the porosity.

3.3.2 PARTICULATES FROM LOOP 8, ON LINE DISTILLATION

The first attempt has been made to concentrate particulate impurities by vaporization of a large sample of loop sodium with the on line distillation system. Operation of the system was generally satisfactory. Seventeen separate additions were made to the distillation cup to provide a one kilogram sample. However, one inadvertant over-fill of the cup was believed to have caused appreciable loss of sample. Only about 7 mg of material, instead of an expected 100 mg were found. The sample contained a relatively large concentration of sodium and calcium and lesser amounts of the stainless steel constituents. X-ray diffraction analyses showed sodium carbonate to be the major constituent. Small amounts of alpha-iron and a compound of the form $NaMO_2$ were also observed. These results are encouraging in that they are generally compatible with data obtained on particulates by other methods in these studies. However, the absence of Na_2O is unexplained but is probably related to the sample loss.

4. TASK IV: CORROSION AND MASS TRANSPORT EFFECTS ON COMPOSITION, STRUCTURE, AND STRUCTURAL INTEGRITY OF CANDIDATE ALLOYS FOR LMFBR AND LOCALIZED ATTACK

4.1 GENERAL

The objective is to obtain effects of mass transfer on corrosion and structural integrity of alloys in flowing sodium systems with temperature differences. Work under this task includes the testing of types 304 and 316 stainless steel to obtain long-term stress-rupture (to 10,000 hours) data. The present test conditions are 1300°F T_{max}, sodium velocities to 17 ft/sec, and controlled sodium purity corresponding to a plugging temperature $< 300°F$.

In addition to the commercial mill annealed grades of types 304 and 316 stainless steel, the carbide agglomerated (CA) condition (1650°F for 24 hours) is included in the experiments. The basis for selecting the CA heat treatment stems from observations made in EBR-II irradiations, where higher residual ductilities were noted for the CA structure after 3×10^{21} nvt ($E > 1$ MeV).

4.2 TESTING OF LMFBR CLADDING

4.2.1 LOOP 4R: STRESS RUPTURE

[Run 4R-2; 10,000 hours, 1300°F (T_{max}), 500°F (ΔT), $< 300°F$ (T_s)]

During the report period, the loop operated at run conditions shown in table 1, except for shutdowns as a result of specimen failures, heater replacement, and a pump replacement. The loop has presently operated at 1300°F with specimens pressurized for ≈ 6000 hours. The results to date are shown in table 9.

4.2.2 LOOP 5R: STRESS RUPTURE

[Run 5R-5; 5000 hours, 1300°F (T_{max}), 500°F (ΔT), $< 300°F$ (T_s)]

During the report period, the loop operated at run conditions except for an 18-day period when flow could not be maintained due to plugging. The loop has presently operated at 1300°F with the pressure applied for 1260 hours.

There have been no specimen failures to date.

TABLE 9

1300°F BIAXIAL STRESS-RUPTURE DATA FROM RUN 4R-2

Material	Initial Hoop Stress (psi)	Time-to-Rupture (h)
304 CA	7000	2188
304 MA	7000	2198
304 MA	7000	2237
304 CA	7000	2263
316 MA	8000	3822
316 MA	8000	4415
304 CA	5000	4500
316 CA	8000	5162
316 CA	8000	5175
304 MA	5000	5187

NOTES: MA – mill annealed
CA – carbide agglomerated, 1650°F for 24 hours

4.2.3 LOOP 6R: STRESS RUPTURE

[Run 6R-4; 10,000 hours, 1150°F (T_{max}), 440°F (ΔT), $< 300°F$ (T_s)]

During the report period, the loop operated at run conditions except for brief shutdowns as a result of specimen failures. The loop has presently operated at 1150°F with the pressure applied for ≈ 2300 hours.

The results to date are shown in table 10.

TABLE 10

1150°F BIAXIAL STRESS-RUPTURE DATA FROM RUN 6R–4

Material	Initial Hoop Stress (psi)	Time-to-Rupture (h)
304 MA	20,000	514
304 MA	20,000	559
316 MA	20,000	639
304 CA	20,000	1662
304 MA	18,000	1710
304 MA	18,000	1947

4.2.4 STRESS-RUPTURE CONTROL TESTS

Stress-rupture tests are being performed at 1300°F in argon on mill annealed and carbide agglomerated types 304 and 316 stainless steel. The tests are being run for the purpose of supplying control data for the tests in flowing sodium. The same heats of material are being tested in both environments, whereby the environmental effect(s) can be delineated.

The results to date are shown in table 11.

The results, plus those for run 4R-2 and the data reported previously from Loop 5R in quarterly report No. 9 (GEAP-10036), are plotted in figures 2 and 3. On the basis of comparison with the control tests, there is a definite decrease in long term stress-rupture properties due to exposure in nonisothermal flowing sodium.

TABLE 11

1300° F BIAXIAL STRESS-RUPTURE DATA IN ARGON

Material	Initial Hoop Stress (psi)	Time-to-Rupture (h)
316 CA	13,000	1584
316 MA	13,000	2415
304 MA	9,000	2511
304 CA	9,000	2727
304 CA	9,000	2895
316 MA	11,000	3183
304 MA	9,000	3373
304 CA	9,000	3389

4.3 LOCALIZED ATTACK SURVEILLANCE

There have been two instances recently of tubing irradiated in EBR-II (under task F of P.A. 10) showing intergranular attack. The first observation [1] was Mark IA driver fuel element C-249-16, clad with type 304 L stainless steel. The second was the FOE capsule tube[2], which was clad with type 304 stainless steel. In both cases, the attack was selective and isolated. It was concluded that the attack of the Mark IA fuel element was associated with a localized increase in carbon concentration.[1]

The major observation of the FOE capsule tube, other than the attack, was the grain boundary precipitates (sensitization). Sensitization had been noted previously on two other type 304 stainless steel task F capsule tubes, which had

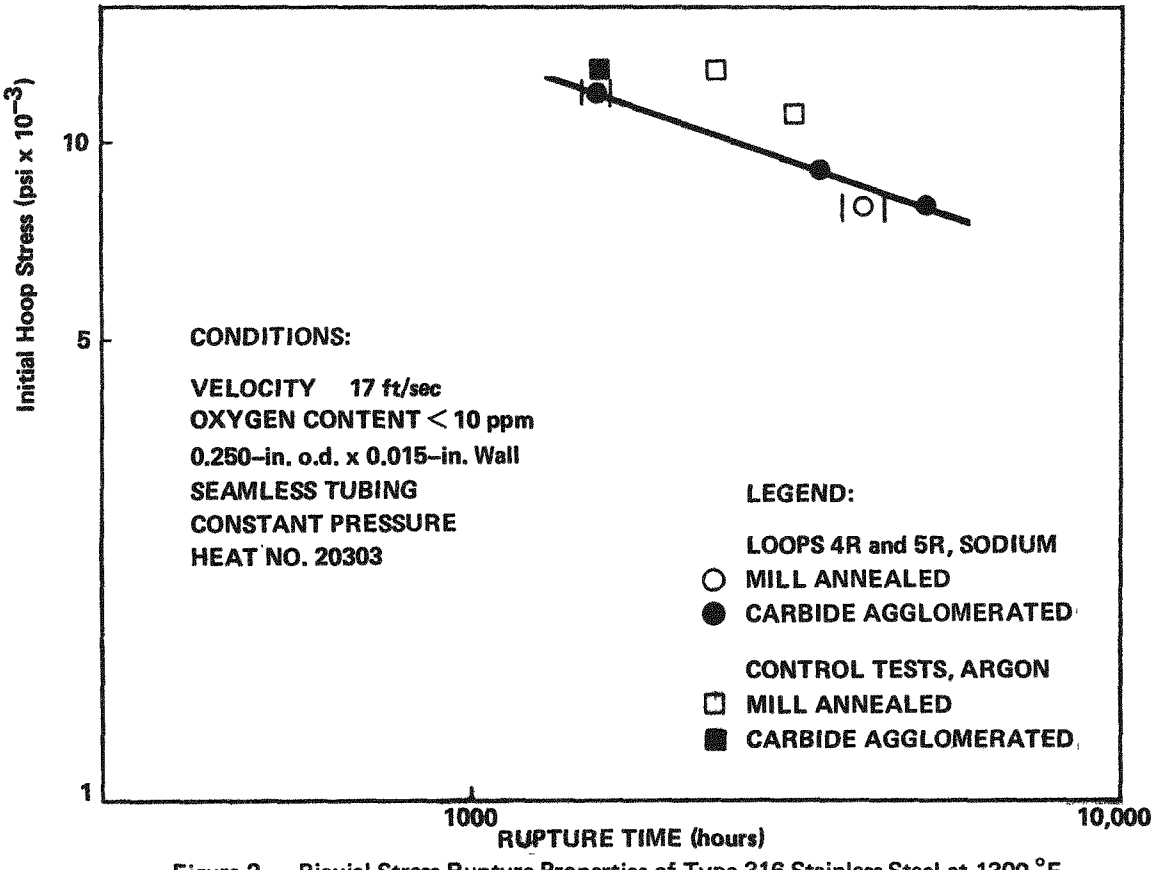

Figure 2. Biaxial Stress Rupture Properties of Type 316 Stainless Steel at 1300 °F

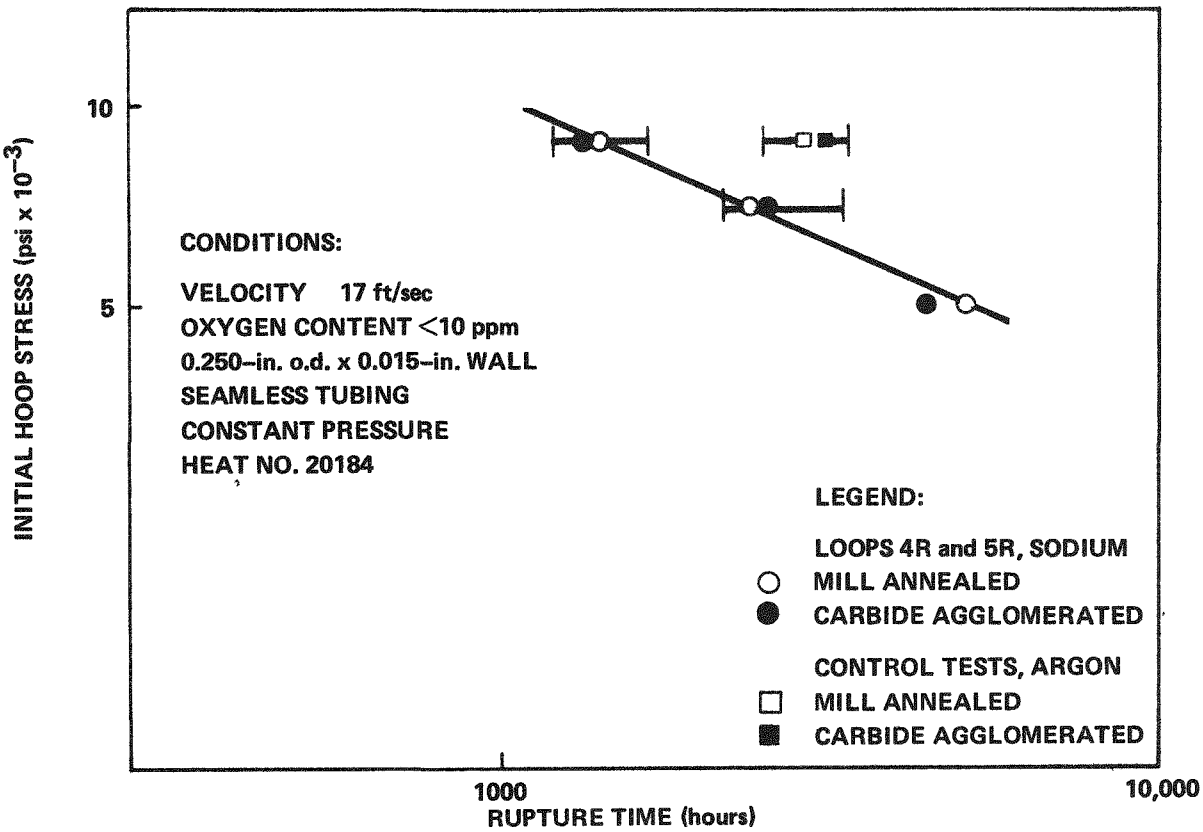

Figure 3. Biaxial Stress Rupture Properties of Type 304 Stainless Steel at 1300°F

been irradiated in EBR-II. The sensitization was not expected for the times and temperatures of exposure. A test was conducted to evaluate the degree of sensitization in task F capsule tubes.

4.3.1 TEST RESULTS

Samples of the sensitized task F capsule tubes were identified as F2Q and F2H. These tubes, as well as capsule tube FOE, were supplied by the Argonne National Laboratory from one heat of type 304 stainless steel (heat No. 136272); see table 12. Some of the pertinent irradiation history of the task F capsules is shown in table 13.

TABLE 12

CHEMICAL COMPOSITION (WT%) OF AISI 304, HEAT NO. 136272

Carbon	0.070
Phosphorus	0.027
Silicon	0.048
Sulfur	0.019
Chromium	18.46
Nickel	9.35
Manganese	1.55
Iron	Balance

TABLE 13

IRRADIATION DATA FOR TASK F CAPSULE TUBES

Capsule	F2Q	F2H	FOE
Months in Core	19	30	37
Peak Fluence (nvt)	1.1×10^{22}	1.4×10^{22}	–
Top of Core Fluence (nvt)	–	0.9×10^{22}	0.6×10^{22}
Average Temp at Core Centerline (°F)	~900	~830	–
Average Temp at Core Top (°F)	–	920	910

The standard ASTM Strauss solution* was chosen to evaluate the degree of sensitization. It had been used previously

* Dissolve 100 g $CuSO_4 \cdot 5H_2O$ in 700 ml distilled water, add 100 ml H_2SO_4 (1.84 sp.gr.), and make up to 1000 ml with distilled water.

to study carbide morphology and its influence on intergranular attack,[3] and also to study the effects of sodium exposure [quarterly report No. 2 (GEAP-5546) and reference 4], such as carburization.

The task F capsule tube, F2U (heat No. 136272), was used in the experiment primarily because of its availability. The F2U capsule tube had a sensitized structure and had been exposed to sodium for 5016 hours in the temperature range of 909° to 927°F. Using an established curve[3] (Figure 4) for type 304 stainless steel susceptibility in the Strauss solution, several heat treatments were chosen to simulate the F2U time-at-temperature exposure. Samples of the original task F capsule tube material (type 304 stainless steel - heat No. 136272) were heat treated at 1000°F for 300 hours, 1100°F for 20 hours, and 1200°F for 2 hours, respectively. The three heat treated samples and an as-received sample were then exposed to the Strauss solution for 24 hours. The as-received sample was not attacked. The heat treated samples had varying degrees of attack, as shown in figures 5, 6 and 7. Several F2U capsule tube samples were exposed separately to the Strauss solution in the RML. The samples disintegrated after 12 hours exposure.

4.3.2 DISCUSSION

The as-received and heat treated original capsule tube material reacted as expected to the Strauss test. The 1000° and 1100°F heat treatments had medium to severe penetration. According to results in figure 4, the attack should have been medium. However, the curve is for a 0.038% C material, and the capsule tube material contained 0.070% C. A higher carbon content would shift the curve to the left. The 1200°F heat treatment produced slight cracking, as predicted from figure 4. On the basis of the results from the heat treated material the F2U capsule tube samples should have had severe penetration due to time at temperature. However, the samples disintegrated, indicating that the sodium exposure had an effect.

Earlier tests [quarterly report No. 2 (GEAP-5546)] have shown that exposure of austenitic stainless steels to carbon contaminated or high carbon sodium will produce disintegration in the Strauss test after five minutes exposure. These samples were sensitized, but did not metallographically shown evidence of a higher carbon concentration. The sensitization was expected, since the exposure temperatures were in the carbide precipitation range. The task F capsule tubes were below the sensitization temperature range, but yet had grain boundary carbides. The observed sensitization plus the disintegration in the Strauss solution indicates a carbon pickup of the task F capsule tubes due to the EBR-II sodium exposure.

The above conclusion agrees with the ANL findings concerning the attacked fuel element, C-249-16[1]. However, the suggestion that local contamination (such as grease) was the source of the carbon pickup is open to question. Several of the F2 capsule tubes had an apparent uniform carbon pickup. The movement of carbon in EBR-II sodium indicated by these observations (cooler-to-hotter areas) is opposite to that observed in test loops. However, the question of local or general carbon pickup becomes subordinate to the question of why carburization of these tubes produce cracking, either during exposure or during removal (cleaning) and storage. To answer this question, an experiment is underway in which the effect of cleaning and storage will be evaluated as it pertains to as-received, heat treated (sensitized), and carburized materials.

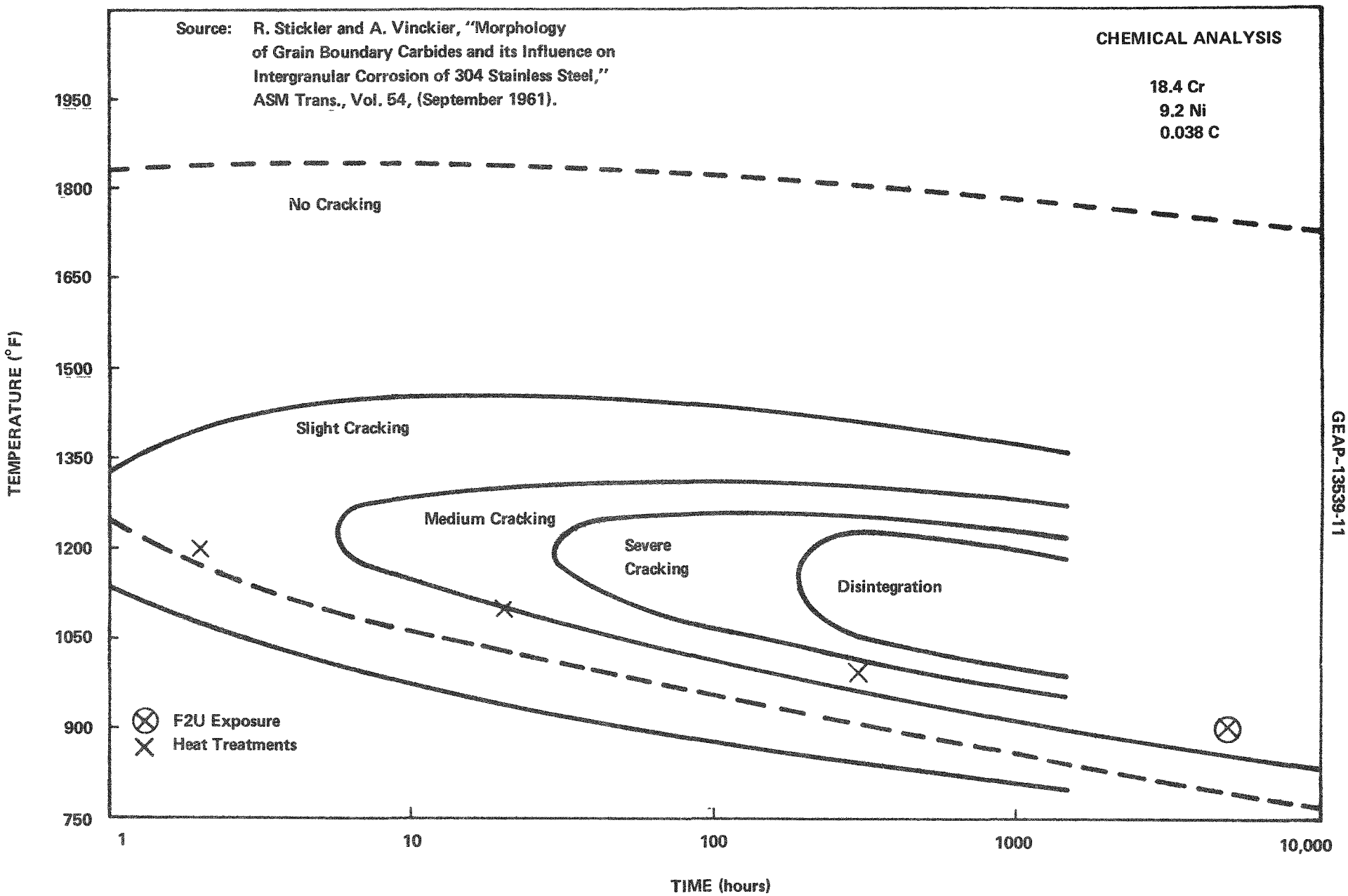

Figure 4. Embrittlement of Sensitized 304 Stainless Steel After A 45-Hour Exposure to Strauss Solution.

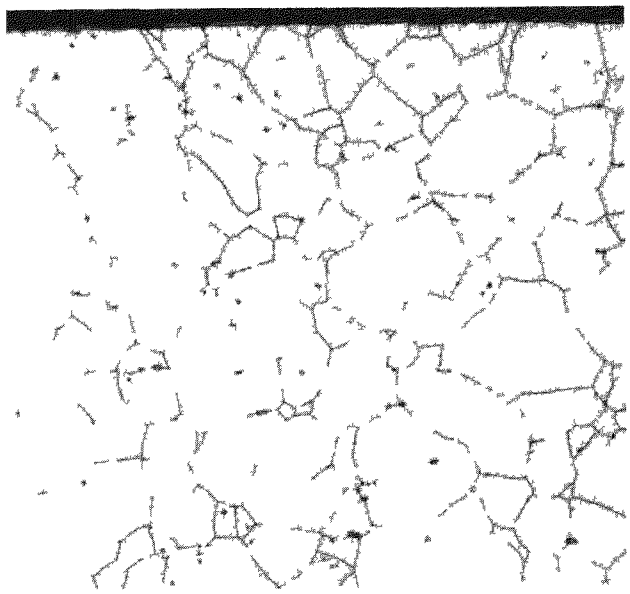

10% Oxalic 500X

Pre–Exposure

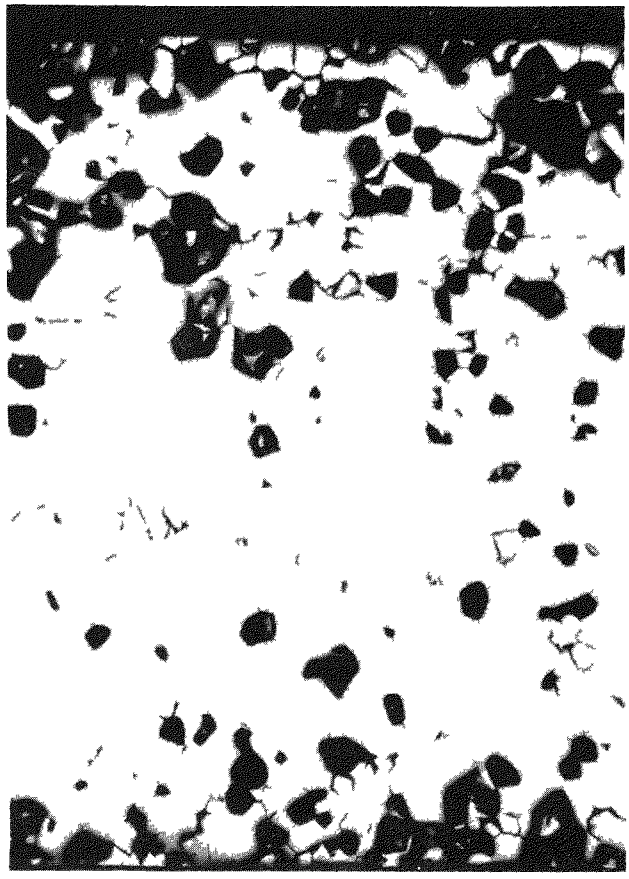

200X

Post–Exposure

Figure 5. Type 304 Stainless Steel Heat Treated at 1000°F for 300 Hours and Exposed to the Strauss Solution for 24 Hours.

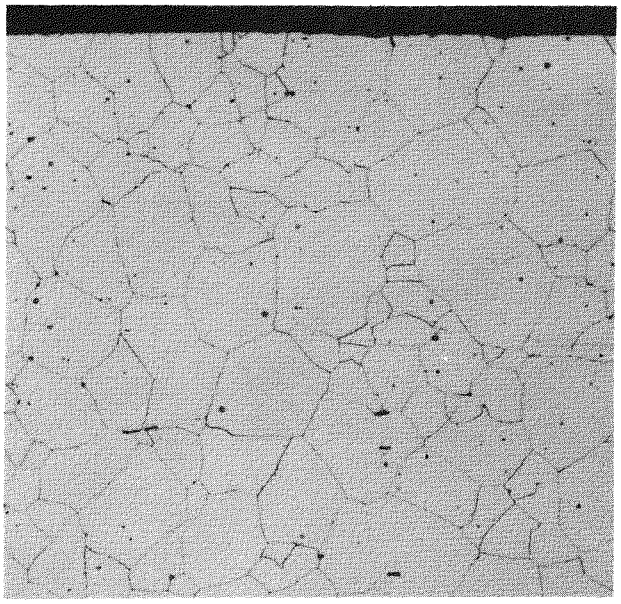

10% Oxalic

500X

Pre–Exposure

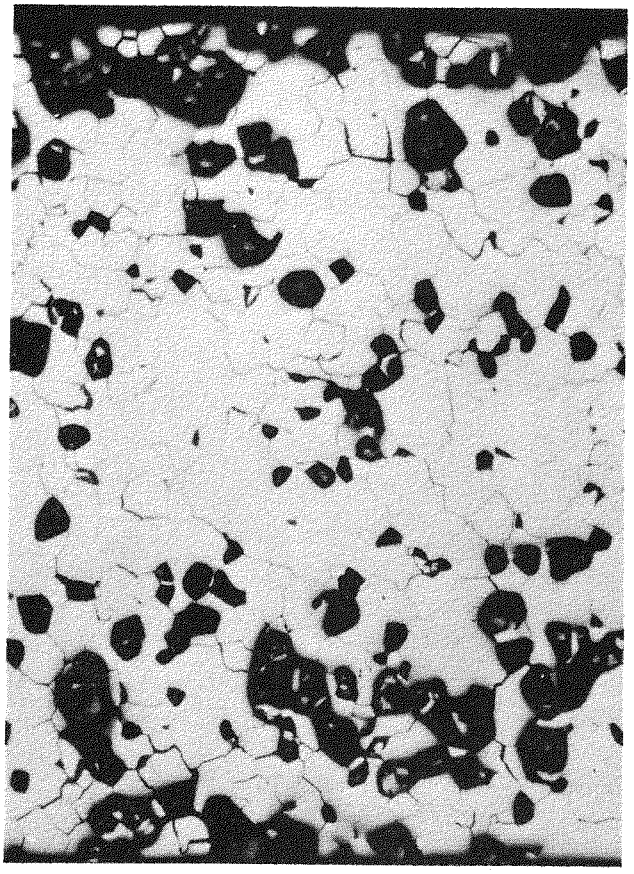

200X

Post–Exposure

Figure 6. Type 304 Stainless Steel Heat Treated at 1100°F for 20 Hours and Exposed to the Strauss Solution for 24 Hours.

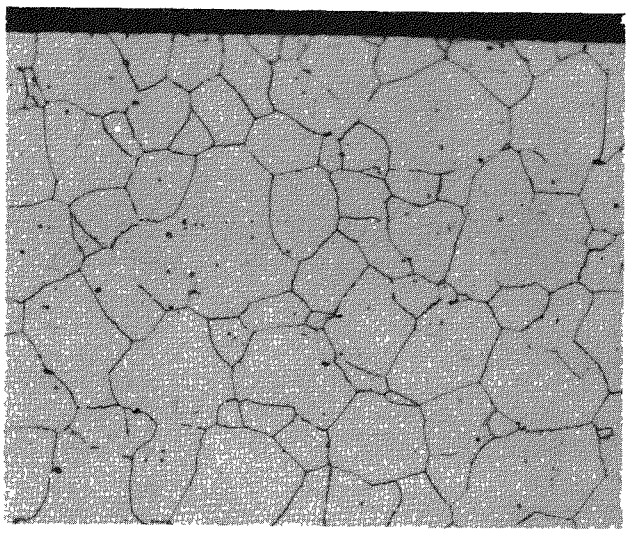

10% Oxalic 500X

Pre–Exposure

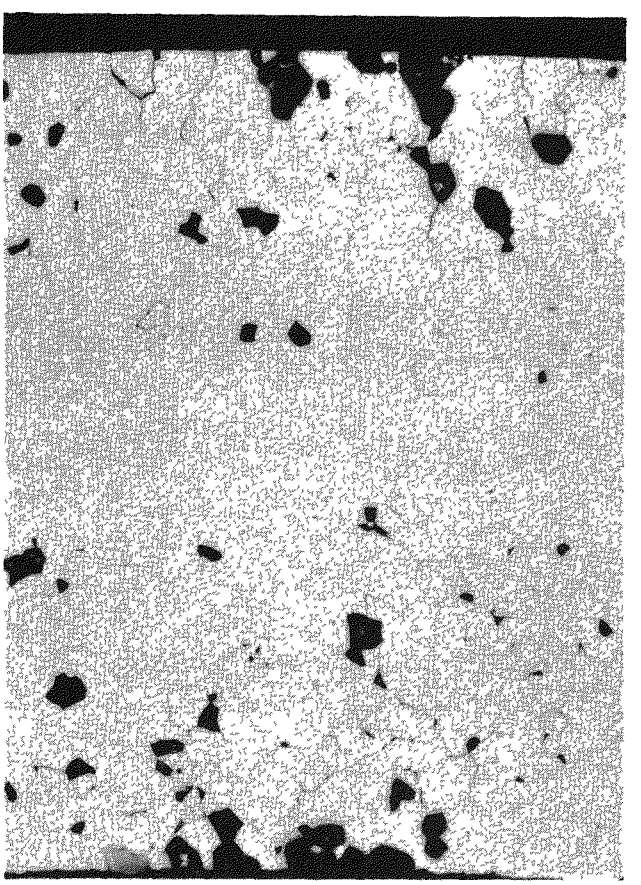

200X

Post–Exposure

Figure 7. Type 304 Stainless Steel Heat Treated at 1200°F for 2 Hours and Exposed to the Strauss Solution for 24 Hours.

5. LIST OF SODIUM MASS TRANSFER PROJECT REPORTS

TOPICAL REPORTS

1. GEAP-3725—Lockhart, R.W., Billuris, G., and Lane, M.R., "Sodium Mass Transfer: I Test Loop Design," June 1962.
2. GEAP-3726—Lockhart, R.W., et al., "Sodium Mass Transfer: II Screening Test Data and Analysis — Mass Transfer Results," Volume I, April 1962.
3. GEAP-3726—Hetzler, F.J., and Young, R.S., "Sodium Mass Transfer: II Screening Test Data and Analysis — Metallurgy," Volume II, June 1962.
4. GEAP-3726—Lockhart, R.W., "Sodium Mass Transfer: I Screening Test Data and Analysis — 1961 Corrosion Sample Data," Volume 3, May 1962.
5. GEAP-4006—Alter, H.W., and McManus, P.A., "Sodium Mass Transfer: III The Application of Liquid Ammonia as a Leaching Agent," April 1962.
6. GEAP-4181—Pohl, L.E., "Sodium Mass Transfer: IV 1962 Corrosion Sample Data," January 1963.
7. GEAP-4182—Lockhart, R.W., "Sodium Mass Transfer: V 1962 Test Run Reports," June 1963.
8. GEAP-4183—Dunn, E.L., "Sodium Mass Transfer: VI Statistical Correlation of 1961 — 1962 Corrosion Data," February 1964.
9. GEAP-4178—Sabol, W.W., and Lockhart, R.W., "Sodium Mass Transfer: VII Methods for Determining Impurities in Sodium Samples," September 1963.
10. GEAP-4313—Mottley, J.D., "Sodium Mass Transfer: VIII Corrosion of Stainless Steel in Isothermal Regions of a Flowing Sodium System," February 1964.
11. GEAP-4436—Lockhart, R.W., et al. "Sodium Mass Transfer: IX The Effect of Carbon and Carbonate Additions in a Sodium Test Loop," December 1964.
12. GEAP-4437—Pohl, L.E., "Sodium Mass Transfer: X 1963 Corrosion Sample Data," February 1964.
13. GEAP-4438—Lockhart, R.W., "Sodium Mass Transfer: XI 1963 Test Run Reports (January - June)," February 1964.
14. GEAP-4439—Lockhart, R.W., "Sodium Mass Transfer: XII 1963 Test Run Reports (July - December), October 1964.
15. GEAP-4540—Sabol, W.W., Dutina D., Rey, D.E., and Simpson, J.L., "Sodium Mass Transfer: XIII The Determination of Total Carbon in Sodium," June 1964.
16. GEAP-4830—Dunn, F.L., Stewart, K.B., and Jaech, J.L., "Sodium Mass Transfer: XIV Statistical Analysis of 1961 - 1964 Sample Weight Change Data," February 1965.
17. GEAP-4831—Rowland, M.C., Plumlee, D.F., and Young, R.S., "Sodium Mass Transfer: XV Behavior of Selected Steels Exposed in Flowing Sodium Test Loops," March 1965.
18. GEAP-4832—Brush, E.G., "Sodium Mass Transfer: XVI The Selective Corrosion Component of Steel Exposed in Flowing Sodium," March 1965.
19. GEAP-4833—Dutina, D., and Simpson, J.L., "Sodium Mass Transfer: XVII The Determination of Hydrogen in Loop Sodium and Cover Gases," June 1965.
20. GEAP-4834—Plumlee, D.E., Lockhart, R.W., and Pohl, L.F., "Sodium Mass Transfer: XVIII Studies of Carbon Movement in Pumped Sodium Test Loops," June 1965.
21. GEAP-4835—Rowland, M.C., Plumlee, D.E., Pohl, L.E., and Lockhart, R.W., "Sodium Mass Transfer: XIX Long-Term Exposure Effects in a Bimetallic Type 316 Stainless Steel - 2-¼ Cr Test Loop," April 1965.
22. GEAP-4836—Pohl, L.E., "Sodium Mass Transfer: XX 1964 Corrosion Sample Data," May 1965.
23. GEAP-4837—Lockhart, R.W., Rowland, M.C., and Pohl, L.E., "Sodium Mass Transfer: XXI 1964 Run Reports," June 1965.
24. GEAP-3838—Rowland, M.C., and Plumlee, D.E., "Sodium Mass Transfer: XXII Metallurgical Examination of the Test Loops," October 1965.
25. GEAP-4602—Lockhart, R.W., Blair, R.C., Dutina, D., Jaech, J.L., and Sabol, W.W., "Results of the USAEC Round-Robin Analysis for Carbon Impurity in Sodium," March 1964.
26. GEAP-5020—Dutina, D., and Simpson, J.L., "Sodium Mass Transfer: XXIV Methods for Separation and Identification of Sodium Impurities," January 1967.

27. GEAP-5560—Steamer, A.G., "Refueling Cell Studies," November 1967.

28. GEAP-4881—Lockhart, R.W., and Blair, R.C., "Sodium Mass Transfer: XVIII, Model for Corrosion Mockup of Sodium Cooled Reactors," July 1967.

29. GEAP-10048—Collins, G.D., "Plugging Indicator Operation," September 1969.

QUARTERLY REPORTS

1. GEAP-4408—"Sodium Components Development Program Mass Transfer Investigations in Liquid Metal Systems, Quarterly Progress Report No. 1, March - May 1967," June 1967.

2. GEAP-5546—"Sodium Components Development Program Mass Transfer Investigations in Liquid Metal Systems, Quarterly Progress Report No. 2, June - August 1967," September 1967.

3. GEAP-5582—"Sodium Components Development Program Mass Transfer Investigations in Liquid Metal Systems, Quarterly Progress Report No. 3, September - November 1967," January 1968.

4. GEAP-5602—"Sodium Components Development Program Mass Transfer Investigations in Liquid Metal Systems, Quarterly Progress Report No. 4, December 1967 - February 1968," May 1968.

5. GEAP-5648—"Sodium Components Development Program Mass Transfer Investigations in Liquid Metal Systems, Quarterly Progress Report No. 5, March - May 1968," July 1968.

6. GEAP-5693—"Sodium Components Development Program Mass Transfer Investigations in Liquid Metal Systems. Quarterly Progress Report No. 6, June - August 1968," October 1968.

7. GEAP-5719—"Sodium Components Development Program Mass Transfer Investigations in Liquid Metal Systems, Quarterly Progress Report No. 7, September - November 1968," January 1969.

8. GEAP-10008—"Sodium Components Development Program Mass Transfer Investigations in Liquid Metal Systems, Quarterly Progress Report No. 8, December 1968 - February 1969," April 1969.

9. GEAP-10036—"Sodium Components Development Program Mass Transfer Investigations in Liquid Metal Systems, Quarterly Progress Report No. 9, March - May 1969," June 1969.

10. GEAP-13539—"Sodium Components Development Program Mass Transfer Investigations in Liquid Metal Systems, Quarterly Progress Report No. 10, June - August 1969," September 1969.

REFERENCES

0. A. W. Thorley and C. Tyzack," Alkali Metal Coolant" Proceedings of the IAEA Symposium on Alkali Metal Coolants, Vienna, Austria, November 1966.
1. W. E. Ruther, T. D. Claar, and S. Matras, *The Attack on the Cladding of EBR-II Driver Fuel Element C-249-16,* Argonne National Laboratory March, 1969, (ANL-7537).
2. GE-BRDO, Sodium-Cooled Reactors, *Fast Ceramic Reactor Development Program, Thirty-First Quarterly Report, May – July 1969,* August 1969, GEAP-10028-31
3. R. Stickler, and A. Vinckier, "Morphology of Grain Boundary Carbides and Its Influence on Intergrandular Corrosion of 304 Stainless Steel," *ASM Trans.,* 54, (September 1961).
4. L. H. Bohne, E. L. Kimont, and F. A. Smith, "Electrical Resistivity Measurement Techniques, A Test for Sodium Exposed Materials Evaluation," *Trans. Am. Nucl. Soc.,* 10, No. 143, (1967).

PROGRAM CONTRIBUTORS

TASK I – LMFBR/FFTF Corrosion Parameter Studies

P. Roy – Task Leader

J. T. Cochran
G. D. Collins
F. A. Comprelli
M. F. Gebhardt
D. W. Jeter
L. E. Pohl
M. K. Schad
J. L. Simpson
G. P. Wozadlo

TASK II – Sodium-Impurities Interactions and Identification of Particulate Matter

D. Dutina – Task Leader

E. A. Aitken
G. D. Collins
R. D. Johnson
J. E. Lewis
L. E. Pohl
P. Roy
J. L. Simpson

TASK IV – Mechanical Properties for Cladding Materials and Localized Attack

G. P. Wozadlo – Task Leader

G. D. Collins
F. A. Comprelli
L. E. Pohl

General Program and Consulting

C. N. Spalaris
R. S. Young
E. L. Zebroski

DISTRIBUTION LIST

John Holliday, Contracts Division
Contract Administration Branch
U. S. Atomic Energy Commission
San Francisco Operations Office
2111 Bancroft Way
Berkeley, California 94704 — 3

Glen W. Wensch, Chief
Liquid Metal Project Branch
Division of Reactor Development and Technology
AEC Headquarters
Washington, D. C. 20545 — 2

Ralph H. Jones, Components Branch
Division of Reactor Development and Technology
AEC Headquarters
Washington, D. C. 20545 — 1

J. A. Lieberman, Asst. Director for Nuclear Safety
Division of Reactor Development and Technology
AEC Headquarters
Washington, D. C. 20545 — 1

S. A. Szawlewicz, Chief
Research and Development Branch
Division of Reactor Development and Technology
AEC Headquarters
Washington, D. C. 20545 — 1

J. M. Simmons, Chief
Fuels and Materials Branch
Division of Reactor Development and Technology
AEC Headquarters
Washington, D. C. 20545 — 1

K. E. Horton
Fuels and Materials Branch
Division of Reactor Development and Technology
AEC Headquarters
Washington, D. C. 20545 — 1

N. Grossman, Chief
Engineering Development Branch
Division of Reactor Development and Technology
AEC Headquarters
Washington, D. C. 20545 — 1

W. R. Kornack
LMFBR Branch
Division of Reactor Development and Technology
AEC Headquarters
Washington, D. C. 20545 — 1

M. J. Whitman
Assistant Director for Program Analysis
Division of Reactor Development and Technology
AEC Headquarters
Washington, D. C. 20545 — 1

L. J. Colby
Chemistry and Chemical Separations Branch
Division of Reactor Development and Technology
AEC Headquarters
Washington, D. C. 20545 — 1

R. Sweek
LMFBR Program Manager, LMFBR Branch
Division of Reactor Development and Technology
AEC Headquarters
Washington, D. C. 20545 — 1

M. Rosen
Assistant Director for Reactor Engineering
Division of Reactor Development and Technology
AEC Headquarters
Washington, D. C. 20545 — 1

J. W. Crawford
Assistant Director for Plant Engineering
Division of Reactor Development and Technology
AEC Headquarters
Washington, D. C. 20545 — 1

J. J. Morabito
Special Projects Branch, FFTF Project
Division of Reactor Development and Technology
AEC Headquarters
Washington, D. C. 20545 — 1

E. E. Sinclair
Assistant Director for Reactor Technology
Division of Reactor Development and Technology
AEC Headquarters
Washington, D. C. 20545 — 1

A. Giambusso
Assistant Director for Project Management
Division of Reactor Development and Technology
AEC Headquarters
Washington, D. C. 20545 — 1

M. Booth, Chief
Systems Engineering Branch
Division of Reactor Development and Technology
AEC Headquarters
Washington, D. C. 20545 — 2

Chief, Administrative Budget
and Program Analysis 1
Division of Reactor Development and Technology
AEC Headquarters
Washington, D. C. 20545

J. H. DeVan 1
Oak Ridge National Laboratory
P. O. Box Y
Oak Ridge, Tennessee 37830

J. White 1
Oak Ridge National Laboratory
Oak Ridge, Tennessee 37830

R. E. MacPherson 1
Oak Ridge National Laboratory
Oak Ridge, Tennessee 37830

D. Gurinsky 2
Brookhaven National Laboratory
Upton, Long Island
New York 11973

Sherman Greenberg, EBR II 1
Argonne National Laboratory
Bldg 212, D107
9700 South Cass Avenue
Argonne, Illinois 60439

F. Smith 1
Argonne National Laboratory
9700 South Cass Avenue
Argonne, Illinois 60439

W. R. Simmons 1
Argonne National Laboratory
LMFBR Program
Office--Bldg 11A
9700 South Cass Avenue
Argonne, Illinois 60439

R. Bane 1
Argonne National Laboratory
Bldg 200, Room B-169
9700 South Cass Avenue
Argonne, Illinois 60439

R. Humphreys, LMFBR Program Office 1
Argonne National Laboratory
9700 South Cass Avenue
Argonne, Illinois 60439

W. R. Wykoff 1
Los Alamos Scientific Laboratory
Los Alamos, New Mexico 87544

G. Waterbury 1
Los Alamos Scientific Laboratory
Los Alamos, New Mexico 87544

L. E. Whinery 1
Los Alamos Scientific Laboratory
Los Alamos, New Mexico 87544

E. R. Astley, FFTF Project Manager 3
Battelle-Pacific Northwest Laboratory
Richland, Washington 99352

Supervisor of Configuration Control 2
FFTF Project
Battelle-Pacific Northwest Laboratory
Richland, Washington 99352

R. W. Dickinson, Director, LMEC 1
Atomics International
P. O. Box 309
Canoga Park, California 91304

J. Droher, Director LMIC 1
Atomics International
P. O. Box 309
Canoga Park, California 91304

Technical Director 2
Atomic Power Development Associates, Inc.
1911 First Street
Detroit, Michigan 48226

R. C. Werner 1
Mine Safety Appliances Research Corp.
Callery, Pennsylvania

Phillip S. Otten 1
Baldwin-Lima-Hamilton Corporation
Eddystone, Pennsylvania 19013

J. H. Wright 1
Westinghouse Corporation
Atomic Power Division
P. O. Box 355
Pittsburgh, Pennsylvania 15230

Paul B. Probert, Project Engineer 1
Babcock & Wilcox Company
Barberton, Ohio 44203

C. A. Barrett
National Aeronautics and Space Administration
Lewis Flight Propulsion Laboratory
Cleveland, Ohio 44135 — 1

Kurt Goldmann
United Nuclear Corporation
White Plains, New York 10601 — 1

RDT Senior Site Representatives
Atomics International
Canoga Park, California 91304
Attn: R. L. Morgan — 1

RDT Senior Site Representatives
General Electric Company
Sunnyvale, California 94086
Attn: J. V. Levy — 1

RDT Senior Site Representatives
Pacific Northwest Laboratory
Richland, Washington 99352
Attn: P. G. Holsted — 1

RDT Senior Site Representatives
Atomic Power Development Associates Inc.
Detroit, Michigan 48226
Attn D. J. Wille — 1

Division of Technical Information Extension
U.S. Atomic Energy Commission
P. O. Box 62
Oak Ridge, Tennessee 37831 — 50

E. C. Bishop
Advance Research Division
Westinghouse Corporation
P. O. Box 158
Madison, Pennsylvania 15663 — 1

Los Alamos Scientific Laboratory
P. O. Box 1663
Los Alamos, New Mexico 87544
Attn: Reports Librarian — 1

S. Golan, Project Manager
1000 MWe LMFBR Follow-On Study
Atomics International
P. O. Box 309
Canoga Park, California 91304 — 2

M. W. Croft, Project Manager
1000 MWe LMFBR Follow-On Study
The Babcock & Wilcox Company
P. O. Box 1260
Lynchburg, Virginia 24505 — 2

W. P. Staker, Project Manager
1000 MWe LMFBR Follow-On Study
Combustion Engineering, Inc.
P. O. Box 500
Windsor, Connecticut 06095 — 2

W. Chernock
Combustion Engineering, Inc.
P. O. Box 500
Windsor, Connecticut — 2

C. A. Anderson, Project Manager
1000 MWe LMFBR Follow-On Study
Westinghouse Electric Corporation
Advanced Reactors Division
Waltz Mill Site
P. O. Box 158
Madison, Pennsylvania 15663 — 2

L. W. Fromm, Manager
1000 MWe LMFBR Follow-On Study Project
Building 208
Argonne National Laboratory
9800 South Cass Avenue
Argonne, Illinois 60439 — 2

Battelle Memorial Institute
Columbus Laboratories
505 King Avenue
Columbus, Ohio 43201
Attn: John E. Davis — 1

L. Kelman
LMFBR Program Office
Argonne National Laboratory
9700 South Cass Avenue
Argonne, Illinois 60439 — 1